Journal of Hydrology 374 (2009) 282–293

Contents lists available at ScienceDirect

Journal of Hydrology

journal homepage: www.elsevier.com/locate/jhydrol

Coherence between lake ice cover, local climate and teleconnections (Lake Mendota, Wisconsin)

Reza Namdar Ghanbari [a], Hector R. Bravo [a,*], John J. Magnuson [b], William G. Hyzer [c], Barbara J. Benson [b]

[a] College of Engineering and Applied Science, University of Wisconsin-Milwaukee, P.O. Box 784, Milwaukee WI 53201-0784, United States
[b] Center for Limnology, University of Wisconsin-Madison, Madison WI 53706-1413, United States
[c] Independent Consultant in Engineering and Applied Science, Janesville, WI 53545-4162, United States

ARTICLE INFO

Article history:
Received 19 June 2008
Received in revised form 9 May 2009
Accepted 16 June 2009

This manuscript was handled by K. Georgakakos, Editor-in-Chief, with the assistance of Ana P. Barros, Associate Editor

Keywords:
Lake ice
Local climate change
Teleconnections
Time series analysis

SUMMARY

Ice duration has shortened and the ice-off date has become earlier for Lake Mendota from 1905 to 2000 as air temperatures have warmed and snowfall has increased. In addition, the ice record has cyclic components at inter-annual and inter-decadal scales. We examined the frequency domain relations between ice, local climate and the teleconnections, Southern Ocean Oscillation (SOI), Pacific Decadal Oscillation (PDO), North Atlantic Oscillation (NAO), and Northern Pacific Index (NP), through a three-tiered analysis of coherence. The coherence results provide evidence of linear relations between the three levels at inter-annual and inter-decadal frequencies. Of the three local climate variables analyzed, namely temperature, snowfall and snow depth, temperature is the variable that most significantly affects ice duration and ice-off date, at both inter-annual and inter-decadal frequencies. The most significant effect of teleconnections on local climate are the effects of PDO on snowfall and snow depth, and SOI on temperature, at inter-annual frequencies, and the effect of NAO on snowfall at inter-decadal frequencies. The teleconnections that most significantly affect ice-cover duration and ice-off date, particularly at inter-decadal frequencies, are the PDO and the NAO. The influence of PDO on ice-cover appears to be transmitted through temperature, while the influence of the NAO appears to be transmitted through temperature and snowfall. A cascading set of links between teleconnections, local climate, and lake ice explain some, but not all, of the dynamics in these time series.

Introduction

Large and persistent ocean–atmospheric anomalies such as the El Niño-Southern Oscillation or ENSO and Pacific Decadal Oscillation or PDO exist over large areas that affect regional climate conditions in adjacent or remote regions. These anomalies are called "teleconnections" (Wallace and Gutzler, 1981). An important aspect of climate change and variability is how teleconnections are related to and influence local climate and ecosystems such as lakes. Physical reasoning and past work indicates that ice cover on lakes should be related to local climate variables, such as air temperature and snow cover, and that local climate and ice cover should be related to teleconnections, whose influence is "transported" to localities away from their source (Robertson, 1989; Mantua and Hare, 2002; Livingstone, 2000; Magnuson et al., 2000, 2003; Hurrell et al., 2003; Bonsal et al., 2006; Tsonis et al., 2006).

Earlier studies in the time domain reveal that these teleconnections have an influence on the ice dynamics of lakes over large regions. Ice-off dates for Lake Mendota, Wisconsin, have been associated with El Niño events (Robertson, 1989; Anderson et al., 1996; Robertson et al., 2000). Relations between ice-off date and the Southern Oscillation Index (SOI) and the North Atlantic Oscillation (NAO) are apparent over portions of 131-year records of five lakes widely scattered across North America and Eurasia using linear regression (Livingstone, 2000). Similarly, ice-off dates were related negatively to the Pacific North American (PNA) and the Western Pacific (WP) indices across broad regions of North America based on 20-year records on 205 lakes (Benson et al., 2000). These relations have been summarized in Magnuson (2002) and Magnuson et al. (2006). Bonsal et al. (2006) observed similar relations using linear regression from 1950 to 1999 for ice-on and ice-off dates for lakes and for rivers but added the spatial pattern of the relations across Canada. Regions of positive and negative relations occurred broadly across Canada, between the six teleconnections and lakes and rivers. In addition, long-term warming trends are apparent in the lake ice records around the Northern Hemisphere (Magnuson et al., 2000) and in Canada (Duguay et al., 2006). Namdar Ghanbari and Bravo (2008) found significant coherence between Great Lakes levels, regional climate and teleconnections. In this study we investigate the applicability of coherence analysis to the ice cover of a single, smaller-scale lake.

* Corresponding author. Tel.: +1 414 229 6756; fax: +1 414 229 6958.
E-mail address: hrbravo@uwm.edu (H.R. Bravo).

0022-1694/$ - see front matter © 2009 Elsevier B.V. All rights reserved.
doi:10.1016/j.jhydrol.2009.06.024

We examine the frequency domain relations between ice cover on Lake Mendota, local climate variables, and four large-scale teleconnections from 1905 to 2000. This is done not by noting that the time series have or do not have similar spectral components but by examining time series coherence among the three levels. Of interest is whether significant coherencies occur in similar frequency ranges in the climate–ice, teleconnections–climate and teleconnections–ice relations.

Background and data

Data analyzed are Lake Mendota ice-cover duration and ice-off date; Madison, Wisconsin local temperature, snowfall, and snow depth; and four teleconnection indices – the Southern Oscillation Index (SOI), the Pacific Decadal Oscillation (PDO), the North Atlantic Oscillation (NAO), and the North Pacific Index (NP). The year of observation for ice data is given as the year of ice off. Correspondingly, we used averages over the winter months (December–March, DJFM) for the Madison local climate variables and the teleconnection data. Coherence relations between ice, local climate, and teleconnections were more significant when using DJFM values than when using full-year averages. The length (Table 1) of each time series made it possible to analyze coherent dynamics from 1905 to 2000 (96 years) among all series and from 1863 to 2000 (137 years) for several series to determine whether the longer records changed the conclusions. All time series data were normalized in terms of their mean and standard deviation.

Lake ice (Fig. 1)

Ice data for Lake Mendota, at Madison, Wisconsin, USA, were selected for analysis because they provide one of the longest uninterrupted historical, lake-ice time series in North America and because earlier analyses using other methods are published. Ice cover data and documentation including definitions are available at the website of the North Temperate Lakes Long Term Ecological Research Program http://lterquery.limnology.wisc.edu/abstract_new.jsp?id=PHYS. Ice duration is the number of days that the lake was completely ice covered and excludes periods when the lake thawed in mid-winter before freezing again.

Local climate at Madison, Wisconsin (Fig. 1)

Local climate variables used were Madison winter air temperature, snowfall, and snow depth from the Wisconsin State Climatology Office http://www.aos.wisc.edu/~sco/index.html. Winter air temperature is derived from the mean monthly air temperature that is based on the daily mean data, that is, the average of the daily maximum and minimum temperatures. Snowfall is the sum of the daily snowfall. Snow depth is the average snow depth on the ground. The values used for year N are the averages of December of year $N-1$ and January, February, and March of year N.

Table 1
The nine time series analyzed for trends and coherencies with the durations of record.

Time series	Record length
Ice-cover duration	1855–2004
Ice-off date	1855–2004
Local temperature	1896–2005
Snowfall	1885–2005
Snow-depth	1905–2005
NAO	1865–2002
NP	1900–2000
PDO	1900–2005
SOI	1866–2004

Background on teleconnections

Many teleconnections have been identified, but combinations of only a small number of patterns can account for much of the interannual variability in the circulation and surface climate (IPCC, 2007). Quadrelli and Wallace (2004) found that many patterns of Northern Hemisphere variability can be reconstructed as linear combinations of the first two Empirical Orthogonal Functions (EOFs) of sea-level pressure (approximately the Northern Annular Mode, NAM, and the PNA) (Quadrelli and Wallace, 2004). Trenberth et al. (2005) analyzed global atmospheric mass and identified four key rotated EOF patterns: the two annular modes (Southern Annular Mode – SAM, and Northern Annular Mode – NAM), a global ENSO (SOI) – related pattern, and a fourth closely related to the North Pacific Index and the PDO, which in turn is closely related to ENSO and the PNA pattern. The most well-known atmospheric/oceanic teleconnections relevant to climate variability in the U.S. include the ENSO, the PNA, the NAO, and the PDO. Chapter 3 in The Physical Science Basis, Working Group I Contribution to the Fourth Assessment Report of the IPCC (2007) offers clear visualizations of these four teleconnections.

Our study analyzes the ENSO, NP (a proxy for PNA, as discussed below), NAO and PDO because they are well-known atmospheric/oceanic teleconnections relevant to climate variability in the US and because previous research suggests they may affect lake ice cover (Robertson et al., 2000; Livingstone, 2000; Magnuson et al., 2005; Bonsal et al., 2006). Teleconnections are best defined by values over a grid, but it is often convenient to devise simplified indices based on key station values (IPCC, 2007). Below we describe each of the four indices we used and provide some background on each.

The Southern Oscillation Index (SOI)

El Niño involves the warming of tropical Pacific surface waters from near the International Date Line to the west coast of South America, weakening the usually strong sea surface temperature (SST) gradient across the equatorial Pacific, with associated changes in ocean circulation (IPCC, 2007). Its closely associated counterpart, the Southern Oscillation (SO) involves changes in trade winds, tropical circulation, and precipitation and is closely related to El Niño and La Niña events. Historically, El Niño events occurred about every three to seven years and alternate with opposite phases of below-average temperatures in the eastern tropical Pacific referred to as La Niña. Changes in the trade winds, atmospheric circulation, precipitation, and associated atmospheric heating generate extra-tropical responses. The ENSO phenomenon is now understood to span the equatorial Pacific and to have opposite phases, and is associated with, simultaneously, droughts in Australia, New Zealand, and southern Africa, and devastating floods in North America, Peru, and Ecuador (Piechota et al., 2006). Strong ENSO years lead to drought conditions in Southeast Asia during the July–September period, with abnormally low rainfall persisting later in the year (Steffen et al., 2004).

Pacific Decadal Oscillation (PDO)

In the North Pacific Ocean, there are decade-scale transitions or regime shifts such as the Pacific Decadal Oscillation (PDO; Mantua et al., 1997) that can fundamentally alter community structure and nutrient dynamics (Fasham, 2003). The Pacific Decadal Oscillation (PDO) is a pattern of ocean variability in the North Pacific similar to ENSO (SOI) in some respects, but it has a much longer cycle (Mantua et al., 1997; Mantua and Hare, 2002). Specifically, it is defined as the standardized difference between sea surface temperatures (SSTs) in the north-central Pacific and Gulf of Alaska. Influences are primarily on precipitation and temperature conditions on the Pacific Northwest, Alaska, Florida, and the North Pacific Islands.

However, the phase of the PDO may be important in enhancing or dampening ENSO impacts on other regions (Piechota et al., 2006).

North Atlantic Oscillation (NAO)

In the North Atlantic Ocean, the NAO influences upper ocean hydrography and biogeochemistry (Fasham, 2003). The North Atlantic Oscillation (NAO) is a major source of inter-annual variability in atmospheric circulation (Hurrell, 1995). It is associated with changes in the westerlies across the North Atlantic onto Europe. An empirical orthogonal function analysis revealed that the NAO is the dominant mode of variability of the surface atmospheric circulation in the Atlantic and accounts for more than 36% of the variance of the mean December–March sea-level pressure field from 20°N to 80°N and 90°W to 40°E from 1899 to 1994. During high NAO winters the westerlies onto Europe are over 8 m s^{-1} stronger than during low NAO winters. Anomalous southerly flow occurs over the eastern United States, and anomalous northerly flow occurs across western Greenland, the Canadian Arctic and the Mediterranean. The NAO has the strongest signature in the winter months (December–March) when its positive (negative) phase enhances (or diminishes) the Iceland Low and Azores High (Hurrell et al., 2003).

North Pacific (NP) index

Wallace and Gutzler's (1981) PNA teleconnection pattern consists of four centers of action in the mid-tropospheric height field, near Hawaii and along the west coast of North America of one sign, and of opposite sign over the north Pacific and southeast United States. According to Trenberth and Hurrell (1994), this has proven to be a useful index, but does not appropriately weight the four centers of the PNA, in which the North Pacific is by far the most prominent in the height field. Trenberth and Hurrell (1994) chose the NP index as a much more robust but simple measure of the circulation in the North Pacific. The NP Index is available since 1899, while the PNA index is available since 1950. Only since the late 1940s have atmospheric data been available that are sufficient in quality and spatial resolution to identify the dominant patterns of climate variability, such as the Pacific North America pattern and the Pacific Decadal Oscillation (Moore et al., 2002). The correlation of the NP index with the PNA index for 5-month averages (November–March) is −0.91 for 1947–1991. We used the NP index in order to analyze coherence with other time series dating back to 1905.

Teleconnections data (Fig. 1)

The SOI is the differences between Tahiti (eastern Pacific) and Darwin (western Pacific) mean sea-level pressure anomalies (Ropelewski and Jones, 1987). Data were obtained from http://jisao.washington.edu/pacs/additional_analyses/soi.html.

The PDO Index is derived as the leading principal component of monthly sea surface temperature anomalies in the North Pacific Ocean, north of 20°N (Mantua and Hare, 2002). Data were obtained from http://jisao.washington.edu/pdo/PDO.latest. "The monthly mean global average SST anomalies are removed to separate this pattern of variability from any "global warming" signal that may be present in the data."

The NAO Index is calculated from the difference of normalized sea-level pressure between Lisbon, Portugal, and Stykkisholmur/Reykjavik, Iceland. The NAO winter index from DJFM was obtained from http://www.cgd.ucar.edu/cas/jhurrell/indices.data.html#naostatmon.

The North Pacific (NP) index is the area-weighted mean sea-level pressure over the region 30–65°N, 160°E–140°W. The NP index was obtained from the website http://www.cgd.ucar.edu/cas/jhurrell/npindex.html.

Methods

The methods of analysis used included trend analysis, estimation of coherency and estimation of cross-correlations.

Trend analysis

The statistical significance of trends was determined using the nonparametric Mann–Kendall test (Press et al., 1988). Kendall's τ uses only the relative ordering of ranks: higher in rank, lower in rank, or the same in rank. Ranks will be higher, lower, or the same if and only if e values are larger, smaller, or equal, respectively. To define τ, one starts with the N data points (x_i, y_i). Now consider all $\frac{1}{2}\ N(N-1)$ pairs of data points, where a data point cannot be paired with itself, and where the points in either order count as one pair. One calls a pair concordant if the relative ordering of the ranks of the two x's (or for that matter the two x's themselves) is the same as the relative ordering of the ranks of the two y's (or for at matter the two y's themselves). One calls a pair discordant if the relative ordering of the ranks of the two x's is opposite from the relative ordering of the ranks of the two y's. If there is a tie in either the ranks of the two x's or the ranks of the two y's, then one does not call the pair either concordant or discordant. If the tie is in the x's, one will call the pair an "extra y pair." If the tie is in the y's, one will call the pair an "extra x pair." If the tie is in both the x's and the x's, one does not call the pair anything at all.

Kendall's τ is then the following simple combination of these various counts:

$$\tau = \frac{\text{concordant} - \text{discordant}}{\sqrt{\text{concordant} + \text{discordant} + \text{extra} - y}\sqrt{\text{concordant} + \text{discordant} + \text{extra} - x}} \tag{1}$$

This must lie between 1 and −1, and that it takes on the extreme values only for complete rank agreement or complete rank reversal, respectively. A positive τ indicates a positive trend and a negative τ a decreasing trend. The larger the value of τ the more consistent the trend is in direction. The test statistic τ measures the monotonic dependence of x on time. More important, Kendall has worked out, from the combinatorics, the approximate distribution of τ in the null hypothesis of no association between x and y. In this case τ is approximately normally distributed, with zero expectation value and a variance of

$$Var(\tau) = \frac{4N + 10}{9N(N-1)} \tag{2}$$

The Z-value for τ in normal distribution is calculated as follows (Helsel and Hirsch, 2002):

$$Z_S = \begin{cases} \frac{\tau - 1}{Var(\tau)} & \text{if } \tau > 0 \\ 0 & \text{if } \tau = 0 \\ \frac{\tau + 1}{Var(\tau)} & \text{if } \tau < 0 \end{cases} \tag{3}$$

The null hypothesis of no trend is rejected at significance level α if $|Z_S| > Z_{Crit}$ where Z_{Crit} is value of the standard normal distribution

with a probability of exceedence of $\alpha/2$. p-Value of the test can be calculated as follows:

$$P\text{-value} = 2 \times (1\text{-one-sided quantile for } Z_S) \quad (4)$$

Estimation of coherency

Our remaining analyses concentrate on linear spectral methods. The analysis of time series through spectral methods provides a way to identify significant oscillations in a record, and allows us to relate those time scales at one level to climate forcing scales at a higher level, that is local climate and lake ice or teleconnections and local climate and lake ice. Spectral methods are effective in delineating important dynamics and relationships between different time series and are popular when the data size (a problem with all modern climate records) inhibits nonlinear analysis (Ghil et al., 2002; Hanson et al., 2004). Based on the length of records used (96 years), signals with frequency $(>48 \text{ years})^{-1}$ are neglected in this study.

We used coherence analysis between time series (Jenkins and Watts, 1968; Bloomfield, 1976) to evaluate trends and oscillations and to quantify the relations between variables of lake ice, local climate, and teleconnections. Coherence analysis, or cross-spectral analysis, may be used to identify variations that have similar spectral properties (high power in the same spectral frequency bands). This method can be thought of splitting the time series into two components: high (H) and low (L) frequencies: $x_t = x_t^{(H)} + x_t^{(L)}$, and $y_t = y_t^{(H)} + y_t^{(L)}$. We may want to know whether the slow components of x and y vary together in some way (Von Storch and Zwiers, 1999).

The cross-spectrum is defined from the covariance function C_{xy}:

$$\Gamma_{xy}(\omega) = \sum_{\tau=-\infty}^{\infty} C_{xy} \exp\{-2\pi i \tau \omega\}, \ \omega \in [-1/2, \ldots, 1/2] \quad (5)$$

This is a complex function where the power is

$$A_{xy}(\omega)^2 = \mathrm{Re}\big(\Gamma_{xy}(\omega)\big)^2 + \mathrm{Im}\big(\Gamma_{xy}(\omega)\big)^2 \quad (6)$$

and the phase is:

$$\Phi_{xy}(\omega) = \tan^{-1}\left(\frac{\mathrm{Im}\big(\Gamma_{xy}(\omega)\big)}{\mathrm{Re}\big(\Gamma_{xy}(\omega)\big)}\right)^2 \quad (7)$$

A cross-spectrum for two similar processes, but with one shifted in time with respect to the other ($x(t)$ and $x(t+\tau)$), gives the same power spectrum as for the same analysis applied to two identical time series, $x(t)$, but instead of a phase difference of zero, the phase is linear in frequency with a slope proportional to the phase shift: $\Phi_{xy}(\omega) = 2\pi\tau\omega$.

The coherence spectrum is analogous to the conventional correlation coefficient and is defined as:

$$\kappa_{xy}(\omega) = \frac{A_{xy}(\omega)^2}{\Gamma_{xx}(\omega)\Gamma_{yy}(\omega)} \quad (8)$$

Estimated coherencies are considered significant at the 99% and 95% level of confidence when they are larger than the critical value T derived from the upper 1% and 5% points of the F-distribution on $(2, d-2)$ degrees of freedom:

$$T = \frac{2F}{d-2+2F} \quad (9)$$

where d is the degrees of freedom associated with the univariate spectrum estimates. Critical T values derived from the upper 1% and 5% of the F-distribution are 0.68 and 0.53, respectively. Peaks in the squared coherency functions larger than those values are significant at the 99% and 95% confidence levels (referred to as highly significant and significant, respectively).

Squared coherency is the frequency domain analogue of correlation. We estimated squared coherency following Jenkins and Watts (1968) and Bloomfield (1976). Coherence measures the linear dependency of the oscillatory components in two detrended signals. While squared coherency does not indicate cause and effect, significant coherence suggests that changes in one series relate to changes in the other series. Coherence analysis is often used in geophysical time series analysis. For example, Kuo et al. (1990) used the squared coherence to test the hypothesis that the increase in atmospheric carbon dioxide is related to observable changes in the climate, and Tsonis et al. (2005) employed it to show coherence between ENSO and global temperature.

The coherence analysis was confirmed by re-doing the analysis using the longest available records for each pair of variables. The estimated peak coherencies occurred at frequencies similar to those reported for the 96-year time series, and the values of peak coherencies were marginally larger or smaller.

Cross-correlations

This article presents the analysis of coherence between 26 pairs of variables. The values of the phase functions between the same 26 pairs of variables, for frequency bands with significant coherence, provide useful information, but the presentation of results becomes complicated. Knowledge of whether an increase in an input series (e.g., snow depth) produces an increase or decrease in an output series (e.g., ice duration) helps to physically interpret the results. With that goal we calculated the cross-correlation functions between the 26 pairs of variables. For the sake of simplicity only the signs of the cross-correlations functions at lag zero are presented.

Given two series $x_1, x_2, \ldots, x_n$ and $y_1, y_2, \ldots, y_n$ we calculated the cross-correlations between x_t and lagged values of y_t (Box et al., 1994):

$$r_{xy}(l) = \frac{\sum_{t=1}^{n-l}(x_t - \bar{x})(y_{t+l} - \bar{y})}{n s_x s_y}, \quad l = 0, 1, \ldots, L \quad (10)$$

where

$$\bar{x} = \frac{\sum_{t=1}^{n} x_t}{n}$$

$$s_x^2 = \frac{\sum_{t=1}^{n}(x_t - \bar{x})^2}{n}$$

and similarly for y.

Results

Trends

Trends of ice-cover duration, ice-off date, and NP are significantly negative while snowfall and local temperature are significantly positive ($p \leqslant 0.05$ in Table 2). Thus, as winter temperatures and snowfall increased over the 96 years, ice-cover duration decreased and ice-off date became earlier. For the coherence analysis the linear trend was subtracted from these five variables. Snow depth, NAO, PDO, and SOI time series had no significant trend. Moore et al. (2002) presented a 301-year snow accumulation record from an ice core at a height of 5340 m above sea level—from Mount Logan, in northwestern North America. They found a positive, accelerating trend in snow accumulation after the middle of the nineteenth century. This trend is paralleled by a warming over northwestern North America which has been associated with secular changes in both the Pacific North America pattern and the Pacific Decadal Oscillation.

Table 2
Nonparametric trends (t) for the nine time series and the statistical significance using the Mann–Kendall test.

Time series	τ-Value	p-Value
Ice-cover duration	−0.275	6×10^{-7}
Ice-off date	−0.222	5×10^{-5}
Local temperature	0.161	5.3×10^{-3}
Snowfall	0.140	2.3×10^{-2}
Snow-depth	0.015	0.83
NAO	0.012	0.83
NP	−0.243	3×10^{-4}
PDO	−0.020	0.75
SOI	−0.072	0.21

Time series coherence

Coherent relations (Figs. 2–4; Tables 3–5) between the three levels of time series from lake ice, to local climate, to teleconnections are grouped by the link represented between levels: climate–ice, teleconnection–climate, and teleconnection–ice. The "climate–ice" link refers to coherent relations between local climate and lake ice. The "teleconnection–climate" link refers to relations between teleconnections and local climate, and "teleconnection–ice" link refers to relations between teleconnections and lake ice.

Twenty three (out of 26 possible) links are statistically significant at the 95% confidence level, including nine links that are significant at the 99% confidence level (Fig. 5). Links significant at the 95% confidence level include "climate–ice" (five links), "teleconnection–climate" (11 links), and "teleconnection–ice" (seven links). These links occur at inter-annual and/or at inter-decadal frequencies. Inter-annual links are more common than inter-decadal links.

Climate–ice (Table 3, Figs. 2 and 5): The local climate–ice cover squared coherency functions revealed the following results:

(a) Highly significant squared coherencies occurred between winter temperature and both the duration of ice cover (squared coherencies = 0.93, 0.75) and the ice-off date (squared coherencies = 0.73, 0.68). These highly significant relations included both inter-annual and inter-decadal frequencies.

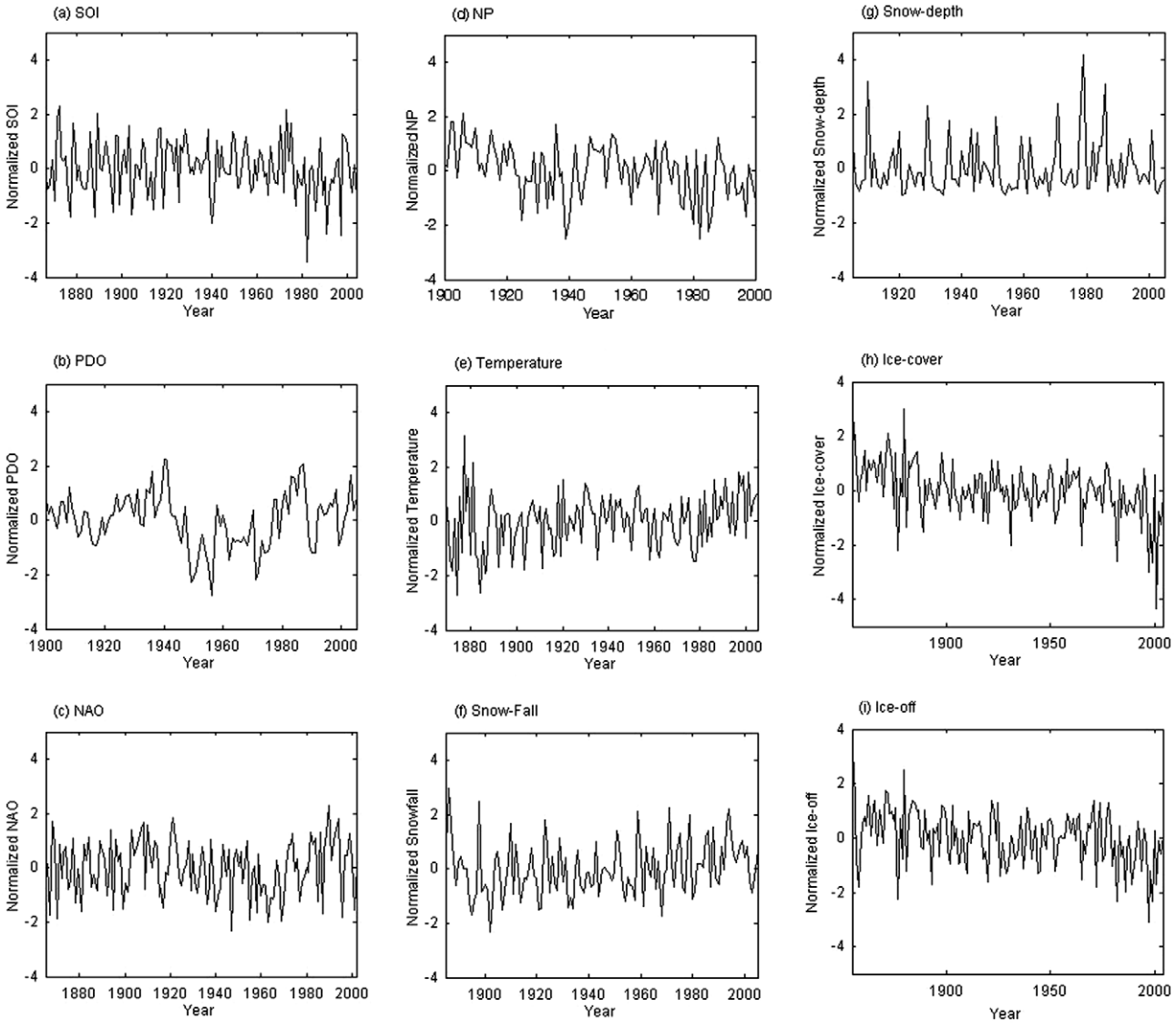

Fig. 1. Normalized time series of (a) SOI, (b) PDO, (c) NAO, (d) NP, (e) local temperature, (f) snowfall, (g) snow depth, (h) ice duration, (i) ice-off date.

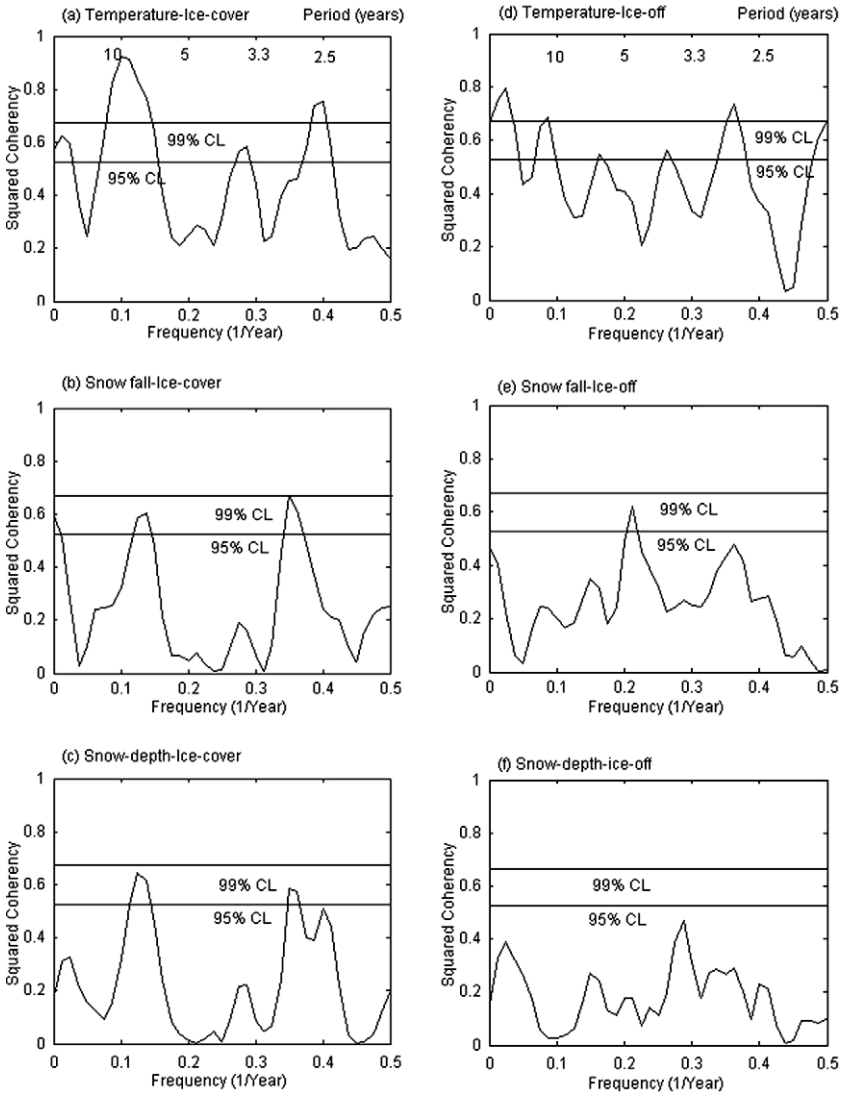

Fig. 2. Climate–ice: graphs of squared coherencies plotted against frequency for relations between lake ice and local climate. Each graph is a pairing of a local climate variable and a lake ice variable. The left column is for relations between local climate and ice-cover duration; the right column is for relations between local climate and ice-off date. The three rows from the top to bottom are for relations between winter air temperature, snowfall, and snow depth, respectively, and lake ice variables. The two horizontal lines represent the 99% or 95% confidence levels.

(b) The squared coherency functions temperature – ice-cover duration and temperature – ice-off date (first row in Fig. 2 and Table 3) have similar shapes, and are more significant than the squared coherencies snowfall – ice cover variables or snow depth – ice cover variables (second and third rows in Fig. 2 and Table 3). The number of significant peaks (at the 95% confidence level) in rows 1, 2 and 3 of Fig. 2 are 8, 4 and 2, respectively.

(c) The squared coherencies between local climate and ice-cover duration (left column in Fig. 2 and Table 3) are more significant than the squared coherencies between local climate and ice-off date (right column in Fig. 3 and Table 4).

(d) The squared coherency function snowfall – ice-cover duration has significant peaks in inter-annual and inter-decadal frequencies, and the squared coherency functions snowfall – ice-off date and snow depth – ice-cover duration have significant peaks in inter-annual frequencies.

Teleconnection–climate (Table 4, Figs. 3 and 5): The teleconnection–climate squared coherency functions showed the following results:

(e) Highly significant squared coherencies between teleconnections and local climate occurred at inter-annual frequencies between SOI and winter temperature (squared coherency = 0.69), PDO and snowfall (squared coherency = 0.86), PDO and snow depth (squared coherence = 0.76). They occurred between NAO and snowfall (squared coherency = 0.77) at inter-decadal frequencies.

(f) The squared coherency functions between PDO and local climate are significant at inter-decadal and inter-annual frequencies. This result, along with result (b) above, suggests that the inter-decadal effect of PDO is transmitted through the local temperature.

(g) The squared coherency functions between NAO and local climate have significant peaks in inter-decadal and inter-annual frequencies. This result, along with result (d) above, suggests that the inter-decadal effect of NAO is transmitted through snowfall.

(h) Additional squared coherency functions that show significant peaks at inter-annual frequencies include: SOI-temperature, SOI-snow depth, NP-temperature, NP-snowfall and NP-snow depth. The SOI – snow depth function also shows a significant peak at inter-decadal frequencies.

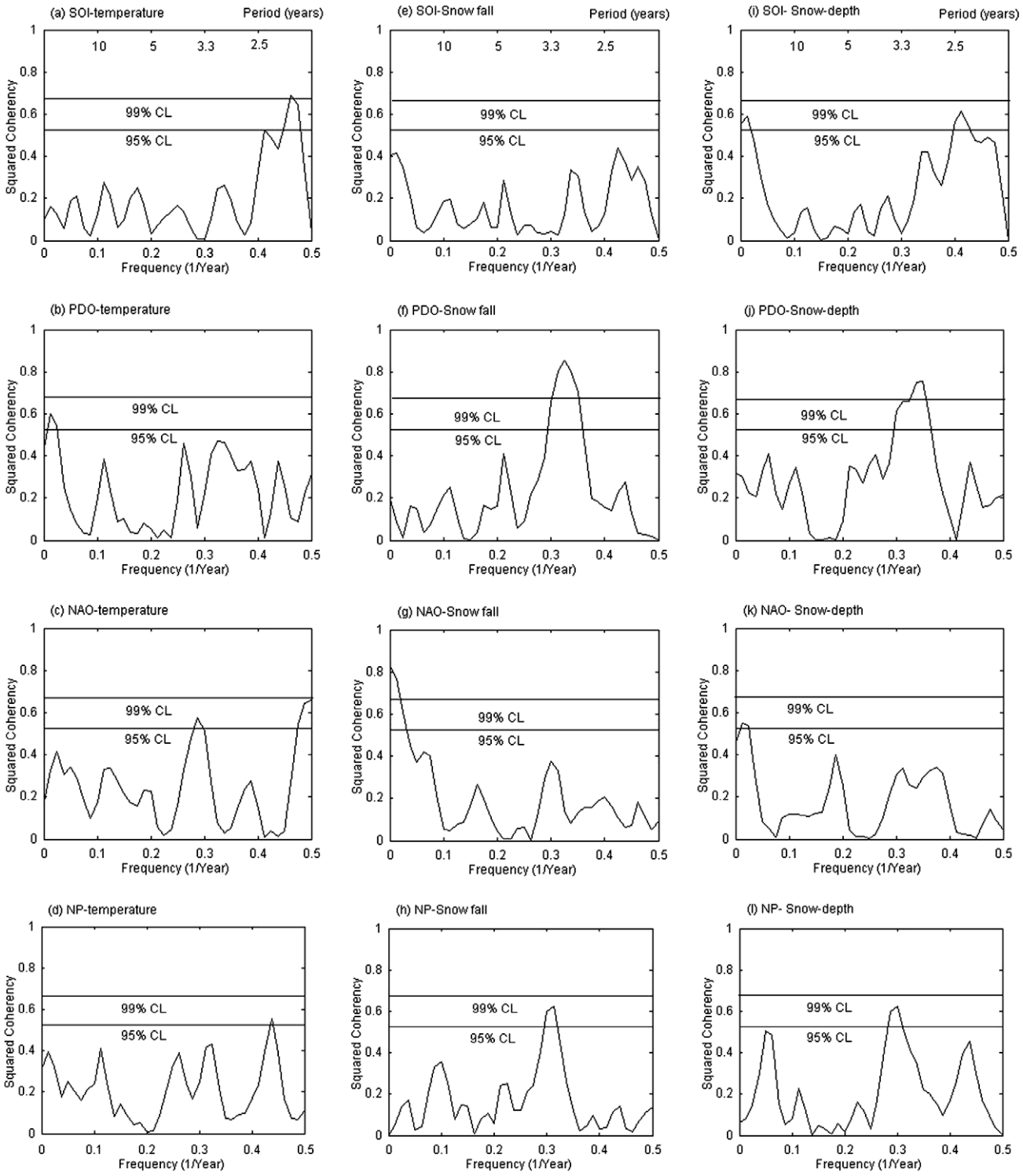

Fig. 3. Teleconnections–climate: graphs of squared coherencies plotted against frequency for relations between teleconnections and local climate. Each graph is a pairing of a teleconnection variable and a local climate variable. The left column is for relations between teleconnections and winter temperature; the center column is for relations between teleconnections and snowfall; the right column is for relations between teleconnections and snow depth. The four rows from the top to bottom are for relations of between SOI, PDO, NAO, and NP, respectively, and local climate. The two horizontal lines represent the 99% or 95% confidence levels.

Teleconnection–ice (Table 5, Figs. 4 and 5): The teleconnection–ice squared coherency functions revealed the following results.

(i) Highly significant squared coherencies between teleconnections and lake ice occurred between PDO and ice-off date (squared coherency = 0.75), and between NAO and both ice-cover duration (squared coherency = 0.76), and ice-off date (squared coherence = 0.72) all at inter-decadal frequencies.

(j) The squared coherency function PDO – ice-cover duration is significant at inter-decadal frequencies and inter-annual frequencies $(5.7–6.2 \text{ years})^{-1}$.

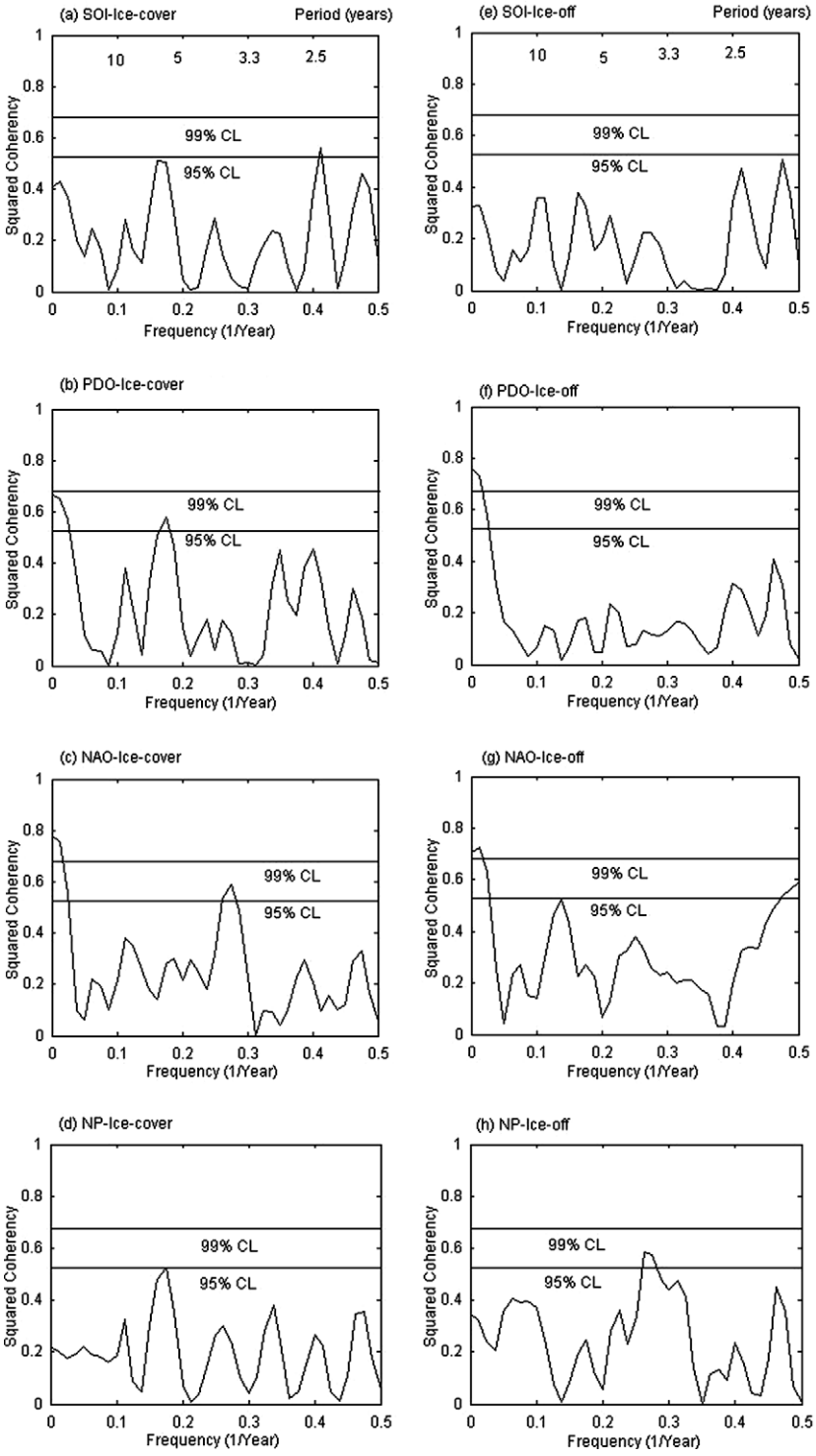

Fig. 4. Teleconnections–ice: graphs of squared coherencies plotted against frequency for relations between teleconnections and lake ice. Each graph is a pairing of a teleconnection variable and a lake ice variable. The left column is for relations between teleconnections and ice-cover duration; the right column is for relations between teleconnections and ice-off date. The four rows from the top to bottom are for relations between SOI, PDO, NAO, and NP, respectively, and lake ice. The two horizontal lines represent the 99% or 95% confidence levels.

(k) The squared coherency functions NAO – ice-cover duration and NAO – ice-off date show significant peaks at inter-annual frequencies: $(3.6–3.8\ \text{years})^{-1}$ and $(7.3\ \text{years})^{-1}$.

(l) The squared coherency function between SOI and ice-cover duration show a narrow significant peak at the inter-annual frequency of $(2.4\ \text{year})^{-1}$.

(m) The squared coherency functions NP – ice-cover duration and NP – ice-off date show a narrow significant peak at $(5.7\ \text{years})^{-1}$ and a significant peak at $(3.6–3.8\ \text{years})^{-1}$, respectively, both inter-annual frequencies.

Table 3
Climate–ice: statistically significant coherencies between local climate (winter air temperature, snowfall, and snow depth) and lake ice (ice-cover duration and ice-off date). Frequency is given as a range of frequencies; squared coherency is given by the maximum value in the frequency range. The (frequency, squared coherency) pairs are ordered by decreasing squared coherency within a climate–ice pair. Bold characters are significant at the 99% confidence level and regular characters at the 95% confidence level.

Local climate variable	Ice-cover duration		Ice-off day	
	Frequency, year^{-1}	Squared coherency	Frequency, year^{-1}	Squared coherency
Local temperature	$(6.7–13.3)^{-1}$	0.93	$(2.7–3.0)^{-1}$	0.73
	$(2.4–2.7)^{-1}$	0.75	$(10.0–13.3)^{-1}$	0.68
	$(3.5–3.6)^{-1}$	0.59	$(3.6–3.8)^{-1}$	0.56
			$(5.7–6.2)^{-1}$	0.55
Snowfall	$(2.8–2.9)^{-1}$	0.67	$(4.7)^{-1}$	0.62
	$(7.3–8.0)^{-1}$	0.61		
	$(>10)^{-1}$	0.57		
Snow depth	$(7.3–8.9)^{-1}$	0.64		
	$(2.8–2.9)^{-1}$	0.59		

Table 4
Teleconnections–climate: statistically significant coherencies between teleconnections (SOI, PDO, NAO, and NP) and local climate (winter temperature, snowfall, and snow depth). Frequency is given as a range of periods; squared coherency is given by the maximum value in the frequency range. The (frequency, squared coherency) pairs are ordered by decreasing squared coherency within a teleconnection–climate pair. Bold characters are significant at the 99% confidence level and regular characters at the 95% confidence level.

Teleconnection	Local temperature		Snowfall		Snow depth	
	Frequency, year^{-1}	Squared coherency	Frequency, year^{-1}	Squared coherency	Frequency, year^{-1}	Squared coherency
SOI	$(2.1–2.2)^{-1}$	0.69			$(2.4–2.5)^{-1}$	0.62
	$(2.4)^{-1}$	0.53			$(>10)^{-1}$	0.60
PDO	$(>10)^{-1}$	0.60	$(2.9–3.3)^{-1}$	0.86	$(2.8–3.3)^{-1}$	0.76
NAO	$(3.3–3.5)^{-1}$	0.58	$(>10)^{-1}$	0.77	$(>10)^{-1}$	0.55
NP	$(2.3)^{-1}$	0.55	$(3.2–3.3)^{-1}$	0.63	$(3.3–3.5)^{-1}$	0.63

Table 5
Teleconnections–ice: statistically significant coherencies between teleconnections (SOI, PDO, NAO, and NP) and lake ice (ice-cover duration and ice-off date). Frequency is given as a range of periods; squared coherency is given by the maximum value in the frequency range. The (frequency, squared coherency) pairs are ordered by decreasing squared coherency within a teleconnection–ice pair. Bold characters are significant at the 99% confidence level and regular characters at the 95% confidence level.

Teleconnection	Ice-cover duration		Ice-off day	
	Frequency, year^{-1}	Squared coherency	Frequency, year^{-1}	Squared coherency
SOI	$(2.4)^{-1}$	0.56		
PDO	$(>10)^{-1}$	0.65	$(>10)^{-1}$	0.75
	$(5.7–6.2)^{-1}$	0.58		
NAO	$(>10)^{-1}$	0.76	$(>10)^{-1}$	0.72
	$(3.6–3.8)^{-1}$	0.59	$(7.3)^{-1}$	0.53
NP	$(5.7)^{-1}$	0.53	$(3.6–3.8)^{-1}$	0.58

Cross-correlations (Table 6)

Cross-correlations at zero lag indicate the direction of the relations between each variable pair. For climate–ice pairings correlations between winter air temperature and both ice-cover duration and ice-off date were negative. Both snow variables were negatively correlated with both ice variables, as well. For teleconnection–climate pairings the correlation between NAO and winter air temperature was positive. The correlation between SOI and temperature was negative. For teleconnection–ice pairings the correlations between NAO with both ice variables were negative. The correlation between SOI and ice-cover duration was positive.

Discussion

The time series of ice cover on Lake Mendota shows a long-term trend related to climate warming and a rich array of inter-annual and inter-decadal cyclic components. These trends in the direction of a warming climate in the Madison area of Wisconsin are consistent with the general warming observed (IPCC, 2007) in the central region of North America. Our results suggest that the cyclic components are influenced by the local climate and teleconnections.

Consider the results of climate–ice coherence (Table 3, Figs. 2 and 5), summarized by results (a)–(d) above. The strongest value of coherence was between air temperature and ice duration at inter-annual and inter-decadal frequencies. The next strongest coherence was between air temperature and ice off at inter-annual and inter-decadal frequencies. All three climatic variables (air temperature, snowfall, and snow depth) were coherent with one or more of the ice-cover measures (ice duration and ice-off date). Not surprisingly, when air temperatures increased, ice duration decreased and ice off occurred earlier.

Analysis of the coherence between teleconnections and local climate (Table 4, Figs. 3 and 5), summarized by results (e)–(h) above indicate that teleconnections may influence ice dynamics through the climatic variables in some cases. The strongest

Table 6
Sign of cross-correlations (at zero lag) between local climate variables and lake ice variables, between teleconnections and local climate variables, and between teleconnections and lake ice variables.

Cross-correlation at zero lag	Ice-cover duration	Ice-off day
Climate–ice		
Temperature	–	–
Snow fall	–	–
Snow depth	–	–

	Temperature	Snow fall	Snow depth
Teleconnection–climate			
SOI	–	+	–
PDO	+	–	+
NAO	+	+	+
NP	–	+	+

	Ice-cover duration	Ice-off day
Teleconnection–ice		
SOI	+	+
PDO	–	–
NAO	–	–
NP	+	+

coherencies at the inter-annual frequencies are between PDO and both snowfall and snow depth and between SOI and air temperature. At the inter-decadal frequencies the strongest relationship is between NAO and snowfall. The zero-lag correlations reveal that as SOI becomes negative or NAO becomes positive air temperature increases and ice duration decreases.

The teleconnections–ice coherence (Table 5, Figs. 4 and 5) was summarized by results (i)–(m) above. The inter-decadal relations with NAO and PDO are the strongest. At inter-annual frequencies ice duration is related to SOI, PDO, NAO, and NP while at inter-decadal frequencies it is influenced by PDO and NAO. Ice-off date is influenced by NAO and NP at inter-annual frequencies and by PDO and NAO at inter-decadal frequencies.

Other authors have found relations between ice cover and the teleconnections. The inter-decadal coherence between PDO and ice duration and ice-off date is consistent with Chao et al. (2000), who identified an inter-decadal oscillation with a period of 15–20 years in the sea surface temperatures over the Pacific Ocean. Our results indicate coherence between PDO and ice cover at inter-annual and inter-decadal frequencies, and between SOI and ice cover at inter-annual frequencies. A study by Rodionov and Assel (2003) examined relations between PDO and the El Niño-Southern Oscillation (ENSO) and both winter temperature in the Laurentian Great Lakes region and surface air temperatures over North America. During warm PDO phases (not coincident with strong El Niño events), atmospheric circulation resembled the classical PNA pattern with a strong Aleutian Low at the surface and amplified ridges and troughs in the mid-troposphere. During strong El Niño events the Aleutian Low is stronger than normal, but shifted eastward, to the Gulf of Alaska. Over North America, a deep trough does not accompany an upper atmospheric ridge on the east as in the classical PNA pattern. Thus, outbreaks of cold Arctic air over the eastern US are rare and winters in the Great Lakes are abnormally mild.

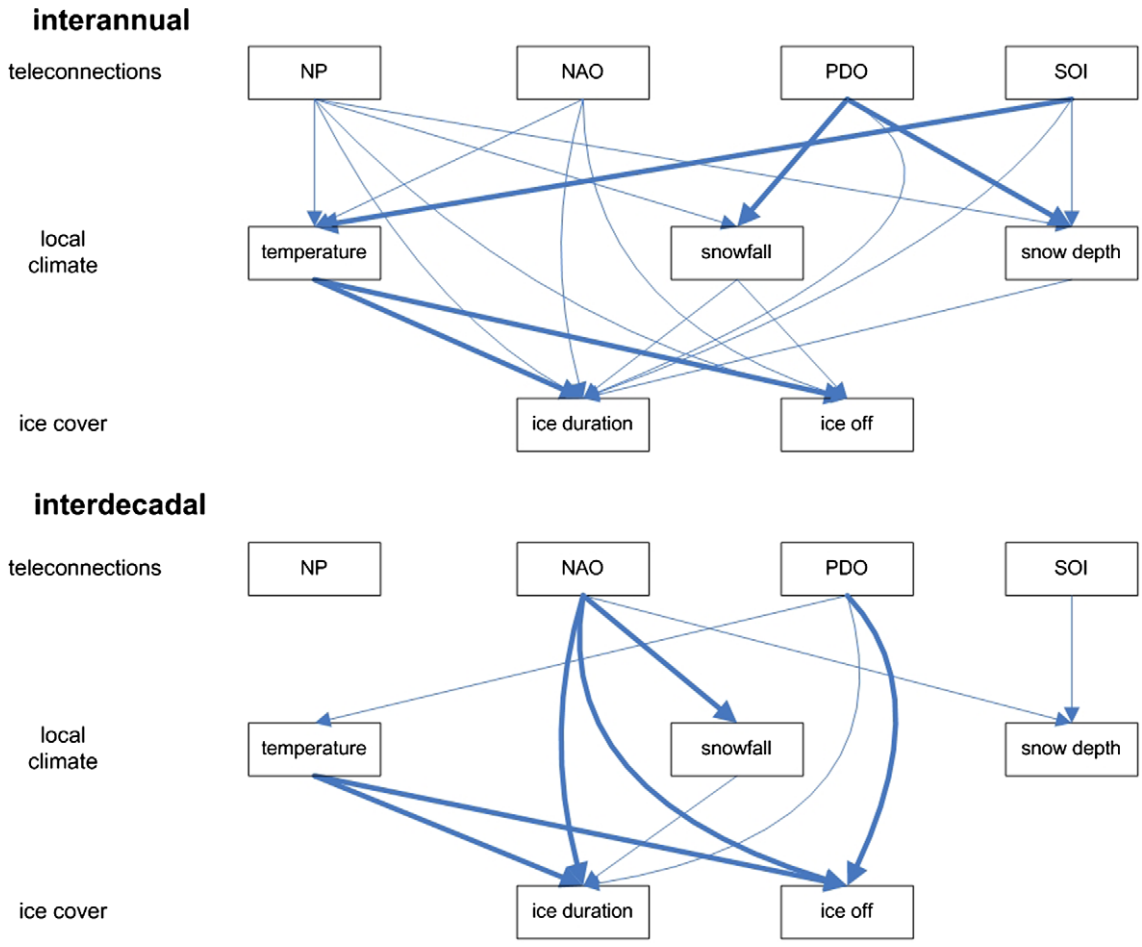

Fig. 5. Diagram of inter-annual relations (top) and inter-decadal relations (bottom) of coherency links among the three levels of variables (two lake ice variables, three local climate variables, and four teleconnection variables). Thick lines are for links significant at the 99% confidence level; thin lines for the 95% confidence level. The arrow points designate the presumed direction of influence.

The inter-decadal coherencies between NAO and ice-cover duration and ice-off date is consistent with Hurrell's (1995) findings on atmospheric circulation and lower tropospheric temperatures during winter over the North Atlantic and adjacent land areas. These temperatures were more strongly linked to the behavior of the NAO than to sea surface temperatures in the tropical Pacific.

For SOI and NP the influences we observed are consistent with the linear correlations for Canadian lakes and streams found by Bonsal et al. (2006); in their study, years with negative values of SOI and NP had later ice-on dates and earlier ice-off dates. Our frequency domain results are consistent with the directional changes in PDO observed by Bonsal et al., because at Lake Mendota higher PDO values were correlated with warmer air temperatures, earlier ice-off dates, and shorter ice cover. For Lake Mendota positive values of NAO were associated with warmer temperatures and less ice. In the Canadian analyses relations of ice-on and -off dates with NAO were only apparent in far eastern Canada. That Lake Mendota shares significant components of its dynamics with NAO and more eastern waters is not surprising. Southern Wisconsin lakes are significantly correlated with New York lakes using linear regression of lake-ice time series (Magnuson et al., 2005), and linear correlations between NAO and Lake Mendota ice-cover have been observed over portions of the two time series using ice-off dates (Livingstone, 2000).

In some cases the climate–ice, teleconnections–climate and teleconnections–ice squared coherency functions were significant at common frequencies. This finding would suggest that in these cases the influence of teleconnections on ice might be transmitted through local climate. In some other cases significant coherence occurred for climate–ice links but were not apparent for the teleconnection–ice links. In other cases other links in the cascade were missing. Such complexity could have many causes related to variables we did not include in the analyses; these may include a variety of other local climate measures, equatorial stratospheric winds (Baldwin et al., 2001), and cyclic changes in solar radiation. Some local climate variables that we did not include may be influenced by the teleconnections such as differences in cloudiness that would alter the radiation reaching the lake's surface among years; and changes in storm frequency and wind strength that could delay ice on (it needs to be cold and calm to freeze over) or result in earlier ice off (push the ice beginning to melt away from the northern shores back and forth against the shorelines with consequent ice shoves and breakup). The later phenomenon occurs in some springs while in other springs the ice basically melts in place and remains intact longer.

The SOI-ice squared coherency functions (Fig. 4) showed several peaks in the $(3–7\ \text{years})^{-1}$ frequency range, but they were not significant at the 95% confidence level. We expected to see significant coherence in that frequency range because earlier analyses clearly pointed out that in the spring following an El Niño event the ice-off date is earlier (Robertson, 1989; Anderson et al., 1996). Explanations for the insufficient significance of the coherence in our frequency-domain analyses over 96 years may be that the relation between Mendota ice-off date differs considerably over this span of years. El Nino caused earlier ice off after 1950 but later ice off prior to 1950 (Robertson et al., 2000).

Namdar Ghanbari and Bravo (2008) analyzed the coherence between teleconnections, regional climate and Great Lakes levels. That analysis yielded squared coherency functions with higher values and broader peaks than the ones presented in this study. We believe that the differences in spatial scales and temporal data resolution (time series of monthly data in the Great Lakes study versus annual data in this ice cover study) explain the observed difference in magnitude and width of coherence peaks. When one considers smaller spatial-scale phenomena such as Lake Mendota ice cover, the influence of local climate, e.g., storm characteristics, grows relative to that of teleconnections.

Concluding remarks

Other researchers found links between teleconnections and lake ice using time domain methods, or comparing spectral characteristics of individual time series. This study found links between teleconnections, local climate and lake ice using coherence analysis, i.e., the simultaneous spectral analysis of pairs of time series.

Our results on coherent dynamics provide significant evidence of the existence of linear relations, at several frequencies, between local climate and ice cover, between teleconnections (SOI, PDO, NAO and NP) and local climate, and between teleconnections and lake ice cover. Of the three local climate variables analyzed, namely temperature, snowfall and snow depth, temperature is the variable that most significantly influences ice duration and ice-off date, at both inter-annual and inter-decadal frequencies. The most significant influence of teleconnections on local climate are those of PDO on snowfall and snow depth at inter-annual frequencies, and SOI on temperature at inter-annual frequencies, and those of NAO on snowfall at inter-decadal frequencies. The teleconnections that most significantly affect ice-cover duration and ice-off date, particularly at inter-decadal frequencies are the PDO and the NAO. Our results suggest that the effect of the PDO on ice cover is transmitted through local air temperature, whereas the effect of the NAO on ice cover is transmitted through snowfall.

While this study found significant coherence between teleconnections, local climate and Lake Mendota ice cover, Namdar Ghanbari and Bravo (2008) found stronger coherence between teleconnections, regional climate and Great Lakes levels. The latter coherences are stronger than the former because of integration and spatial scales issues. Furthermore, the results of both studies suggest that the patterns of ice cover in Lake Mendota might share characteristics with other lakes in the region owing to the large footprint of the teleconnections.

Acknowledgements

This study was partially funded through a grant from State of Wisconsin Groundwater Coordinating Council and the USGS Ground-Water Resources Program and the National Science Foundation through the North Temperate Lakes Long-Term Ecological Research Program. Anastasios Tsonis provided invaluable comments to an earlier version of this manuscript.

References

Anderson, W.L., Robertson, D.M., Magnuson, J.J., 1996. Evidence of recent warming and El-Niño-related variations in ice break-up of Wisconsin lakes. Limnology and Oceanography 41, 815–821.

Baldwin, M.P., Gray, L.J., Dunkerton, T.J., Hamilton, K., Haynes, P.H., Randel, W.J., Holton, J.R., Alexander, M.J., Hirota, I., Horinouchi, T., Jones, D.B.A., Kinnersley, J.S., Marquardt, C., Sato, K., Takahasi, M., 2001. The quasi-Biennial oscillation. Reviews of Geophysics 39 (2), 179–229.

Benson, B.J., Magnuson, J.J., Jacob, R.L., Fuenger, S.L., 2000. Response of lake ice breakup in the Northern Hemisphere to the 1976 interdecadal shift in the North Pacific. Verhandlungen Internationale Vereinigung für Theoretische und Angewandte Limnologie 27, 2770–2774.

Bloomfield, P., 1976. Fourier Analysis of Time Series: An Introduction. Wiley.

Bonsal, B.R., Prowse, T.D., Duguay, C.R., Lacroix, M.P., 2006. Impacts of large-scale teleconnections on freshwater-ice break/freeze-up dates over Canada. Journal of Hydrology 330, 340–353.

Box, G.E.P., Jenkins, G.M., Reinsel, G.C., 1994. Time Series Analysis: Forecasting and Control, third ed. Prentice Hall.

Chao, Y., Ghil, M., McWilliams, J.C., 2000. Pacific interdecadal variability in this century's sea surface temperatures. Geophysics Research Letters 27 (15), 2261–2264.

Duguay, C.R., Prowse, T.D., Bonsal, B.R., Brown, R.D., Lacroix, M.P., Ménard, P., 2006. Recent trends in Canadian lake ice cover. Hydrological Processes 20, 781–801.

Fasham, M.J.R. (Ed.), 2003. Ocean Biogeochemistry: The Role of the Ocean Carbon Cycle in Global Change Global Change – The IGBP Series. Springer.
Ghil, M., Allen, M.R., Dettinger, M.D., Ide, K., Kondrashov, D., Mann, M.E., Robertson, A.W., Saunders, A., Tian, Y., Varadi, F., Yiou, P., 2002. Advanced spectral methods for climatic time series. Reviews of Geophysics 40, 1.
Hanson, R.T., Newhouse, M.W., Dettinger, M.D., 2004. A methodology to assess relations between climatic variability and variations in hydrologic time series in the southwestern United States. Journal of Hydrology 287, 252–269.
Helsel, D.R., Hirsch, R.M., 2002. Statistical Methods in Water Resources. US Geological Survey. <http://water.usgs.gov/pubs/twri/twri4a3>.
Hurrell, J.W., Kushir, Y., Ottersen, G., Visbeck, M. (Eds.), 2003. The North Atlantic Oscillation, Climatic Significance and Environmental Impact. American Geophysical Union, Washington, DC.
Hurrell, J.W., 1995. Decadal trends in the North Atlantic oscillation: regional temperatures and precipitation. Science 269, 676–679.
Intergovernmental Panel on Climate Change, 2007. Climate Change 2007 – The Physical Science Basis. Working Group I Contribution to the Fourth Assessment Report of the IPCC. Cambridge University Press.
Jenkins, G.M., Watts, D.G., 1968. Spectral Analysis and its Applications, Holden Day.
Kuo, C., Lindberg, C., Thomson, D.J., 1990. Coherence established between atmospheric carbon dioxide and global temperature. Nature 343.
Livingstone, D.M., 2000. Large-scale climatic forcing detected in historical observations of lake ice break-up. Verhandlungen Internationale Vereinigung für Theoretische und Angewandte Limnologie 27, 2775–2783.
Magnuson, J.J., Benson, B.J., Jensen, O.P., Clark, T.B., Card, V., Futter, M.N., Soprano, P.A., Stewart, K.M., 2005. Persistence of coherence of lake ice-off dates for inland lakes across the Laurentian Great Lakes. Verh. International Vereins Limnology 29 (1), 521–527.
Magnuson, J.J., Robertson, D.M., Benson, B.J., Wynne, R.H., Livingston, D.M., Arai, T., Assel, R.A., Barry, R.G., Card, V., Kuusisto, E., Granin, N.G., Prowse, T.D., Stewart, K.M., Vuglinski, V.S., 2000. Historical trends in lake and river ice cover in the northern hemisphere. Science 289, 1743–1746.
Magnuson, J.J., Krohelski, J.T., Kunkel, K.E., Robertson, D.M., 2003. Wisconsin's waters and climate: historical changes and possible futures, in Wisconsin's waters: a confluence of perspectives. Transactions of the Wisconsin Academy of Sciences, Arts and Letters 90, 23–36.
Magnuson, J.J., 2002. Signals from ice cover trends and variability. In: McGinn, N.A. (Ed.), Fisheries in a Changing Climate, vol. 32. American Fisheries Society, Symposium, Bethesda, MD, pp. 3–13.
Magnuson, J.J., Benson, B.J., Lenters, J.D., Robertson, D.M., 2006. Climate driven variability and change. In: Magnuson, J.J., Kratz, T.K., Benson, B.J. (Eds.), Long-term Dynamics of Lakes in the Landscape: Long-term Ecological Research on North Temperate Lakes. Oxford University Press, pp. 123–150.
Mantua, N., Hare, S.R., 2002. The Pacific decadal oscillation. Journal of Oceanography 58 (1), 35–44.
Mantua, N., Hare, S., Zhang, Y., Wallace, J.M., Francis, R., 1997. A Pacific interdecadal climate oscillation with impacts on Salmon production. Bulletin of American Meteorological Society 78, 1069–1079.
Moore, G.W.K., Holdsworth, G., Alverson, K., 2002. Climate change in the North Pacific region over the past three centuries. Nature 420, 401–403.
Namdar Ghanbari, R., Bravo, H.R., 2008. Coherence between teleconnections, regional climate and Great Lakes levels. Advances in Water Resources. doi:10.1016/j.advwatres.2008.05.002.
Piechota, T.C., Garbrecht, J.D., Schneider, J.M., 2006. Climate variability and climate change. In: Garbrecht, J.D., Piechota, T.C. (Eds.), Climate Variations, Climate Change, and Water Resources Engineering. ASCE.
Press, W.H., Flannery, B.P., Teukolski, S.A., Vettering, W.T., 1988. Numerical Recipes: The Art of Scientific Computing. Cambridge Univ Press, New York. 818pp..
Quadrelli, R., Wallace, J.M., 2004. A Simplified linear framework for interpreting patterns of Northern Hemisphere wintertime climate variability. Journal of Climate 17, 3728–3744.
Robertson, D. M. (1989). The use of lake water temperature and ice cover as climatic indicators. Ph.D. Thesis, Oceanography and Limnology Graduate Program, University of Wisconsin-Madison.
Robertson, D.M., Wynne, R.H., Chang, W.Y.B., 2000. Influence of El Niño on lake and river ice cover in the Northern Hemisphere from 1900 to 1995. Verhandlungen Internationale Vereinigung für Theoretische und Angewandte Limnologie 27, 2784–2788.
Rodionov, S., Assel, R.A., 2003. Winter severity in the Great Lakes region: a tale of two oscillations. Climate Research 24, 19–31.
Ropelewski, C.F., Jones, P.D., 1987. An extension of the Tahiti-Darwin southern oscillation index. Monthly Weather Review 115, 2161–2165.
Steffen, W., Sanderson, A., Jäger, J., Tyson, P.D., Moore III, B., Matson, P.A., Richardson, K., Oldfield, F., Schellnhuber, H.-J., Turner II, B.L., Wasson, R.J., 2004. Global Change and the Earth System: A Planet Under Pressure. Springer Verlag, Heidelberg, Germany.
Trenberth, K.E., Stepaniak, D.P., Smith, L., 2005. Interannual variability of patterns of atmospheric mass distribution. Journal of Climate 18 (15), 2812–2825.
Trenberth, K.E., Hurrell, J.W., 1994. Decadal atmosphere–ocean variations in the Pacific. Climate Dynamics 9, 303–319.
Tsonis, A.A., Elsner, J.B., Hunt, A.G., Jagger, T.H., 2005. Unfolding the relation between global temperature and ENSO. Geophysics Research Letters. doi:10.1029/2005GL022875.
Tsonis, A.A., Swanson, K.L., Roebber, P.J., 2006. What do networks have to do with climate? Bulletin of the American Meteorological Society. doi:10.1175/BAMS-87-5-585.
Von Storch, H., Zwiers, F.W., 1999. Statistical Analysis in Climate Research. Cambridge University Press, Cambridge. 484pp. ISBN 0521 450713.
Wallace, J.M., Gutzler, D.S., 1981. Teleconnections in the geopotential height field during the Northern Hemisphere winter. Monthly Weather Review 109, 784–812.